# VELOCITY DEPENDENCE OF 2.5D TRUE-AMPLITUDE SINGLE-STACK REDATUMING

*F. Oliveira, A. Novais, J. Schleicher, and J. Costa*

**email:** *js@ime.unicamp.br*

**keywords:** *Redatuming, velocity, configuration transformation*

**ABSTRACT**

*The objective of this work is to demonstrate the application of single-stack redatuming. The purpose of this operation is to transform seismic data acquired in a certain measurement level, in order to simulate data as if acquired at another level. Recent theoretical advances allow to perform this transformation for zero-offset data in a single step. It consists of performing a single weighted stack along adequately chosen stacking lines. In this work, we demonstrate the application of this method to synthetic seismic data for media with two or many flat layers and in models with lateral velocity variations. In the first case the data are generated at and redatumed to flat surfaces, in the second situation both surfaces of acquisition and redatuming have different topographies, and in the third experiment data from a laterally varying medium are redatumed to a flat datum using only velocity information in the top layer. Moreover, we quantitiatively discuss the dependence of the operator on the velocity model. Our examples demonstrate the quality of the redatumed data both kinematically and dynamically.*

## INTRODUCTION

Redatuming is used with the objective to transform seismic data acquired at a certain measurement level to simulate data as if acquired at another level (Wapenaar et al., 1992). The standard way of realizing a redatuming is by downward continuation of seismic time data (Berryhill, 1979, 1984, 1986). The main goal when using redatuming is to improve the data quality. In practice, redatuming is frequently used to remove the interference of topography from the data, simulating the acquisition at a planar datum. However, the general ideas of redatuming are not restricted to the datum being planar. The general redatuming formalism can include topography at both the original acquisition surface and the new datum.

Over the years, many attempts have been made to achieve the goal of determining the seismic data at a new datum. Wapenaar et al. (1992) proposed a one-way Kirchhoff-Helmholtz extrapolation. Other contributions to the theory of wave-equation-based redatuming methods include the works of Yilmaz and Lucas (1986), Bevc (1997), and Schneider et al. (1995). Schuster and Zhou (2006) provide a comprehensive summary about the state of the art in redatuming

As geometrically discussed by Hubral et al. (1996) and mathematically shown by Tygel et al. (1996), redatuming is a true-amplitude configuration transform (particular case), developed from chaining of diffraction stack migration and isochron stack demigration (Pila et al., 2007b,a).

In practice, redatuming is often only employed kinematically, without regard to preserving the amplitudes. However, when we want to use the dynamic information, for instance in a subsequent true-amplitude migration (see, e.g., Schleicher et al., 1993; Hanitzsch et al., 1994), amplitude preservation is of fundamental importance in the complete processing sequence, including redatuming. In this work, we demonstrate the application of true-amplitude single-stack redatuming to synthetic seismic data for media with two or many flat layers and in models with lateral velocity variations. Moreover, we discuss the dependence of the single-stack redatuming operation on the velocity model. We quantify the kinematic and dynamic error as a function of the error in the velocity model.

## METHODOLOGY

Redatuming is one of the many imaging operations that can be described by chaining Kirchhoff-type migration and demigration integrals. For this purpose, all that has to be done is to interchange the order of integrations and analytically evaluate the new inner integrals. In this way, many one-step imaging operations of the type of a diffraction stack can be developed (Schleicher et al., 2007).

In this work, we study a 2.5D true-amplitude redatuming, i.e., we study the amplitude behavior when redatuming data. The attribute 2.5D (Bleistein, 1986) indicates that in our experiments we consider 3D wave propagation in a 2D earth model. The velocity is invariable in the $y$ direction and the seismic line is positioned along the $x$-axis.

In the analysis below, the location of the source-receiver positions along the original seismic line on the acquisition surface $\mathcal{Z}_o$ is described by their horizontal midpoint coordinate $\xi$. In other words, the original sources and receivers are located at the points $S = (\xi - h, 0, \mathcal{Z}_o(\xi - h))$ and $G = (\xi + h, 0, \mathcal{Z}_o(\xi + h))$, where $h$ is the half-offset. Correspondingly, the simulated source-receiver positions on the new datum $\mathcal{Z}_r$ are described by their horizontal midpoint coordinate $\eta$. The numerical experiments below only consider the zero-offset situation, i.e., $h = 0$ m, with sources and receiver in the same position and equally spaced along the $x$-axis.

We know that for each point ($\eta$,$\tau$) in the redatumed section to be constructed, there is a weighted diffraction-stack operation along problem-specific stacking surfaces, the so-called inplanats $t = \mathcal{T}_r(\xi; \eta, \tau)$, that achieves the desired true-amplitude transformation. Accordingly, the simulated data at a new level can be expressed as a single stacking operator with a weight function $W_r(\xi; \eta, \tau)$ acting upon the input data, i.e.,

$$U_r(\eta, \tau) = \frac{1}{\sqrt{2\pi}} \int_A d\xi \, W_r(\xi; \eta, \tau) \, D^{1/2}[U(\xi, t)]|_{t=\mathcal{T}_r(\xi;\eta,\tau)} \, , \tag{1}$$

where $U(\xi, t)$ stands for the input data and $U_r(\eta, \tau)$ represents the redatumed output data. Moreover, $A$ denotes the aperture of the stack, that is, the region over which data are stacked to contribute to the output value at $(\eta, \tau)$. Finally, $D^{1/2}$ is the half-derivative operation which helps to correctly recover the pulse shape of the source wavelet. It can be represented as

$$D^{1/2}[f(t)]| = \mathcal{F}^{-1} \left[ |\omega|^{\frac{1}{2}} e^{-i \frac{\pi}{2} \mathrm{sgn}\,(\omega)} \mathcal{F}[f(t)] \right] , \tag{2}$$

where $\mathcal{F}$ denotes the Fourier transform.

## STACKING CURVE AND WEIGHT FUNCTION

The determination of the stacking curve is related to the kinematic properties of the problem. The stacking line connects all point in the input section where a reflection event might have been recorded that would appear in the redatumed section at an output point $(\eta, \tau)$. On the other hand, the weight function is related to the amplitude behaviour. The condition for a true-amplitude weight function is that, asymptotically, the simulated reflections must have the same geometrical-spreading factor that the reflections would have if they were actually acquired on the new datum. As shown by Pila et al. (2007b), the resulting true-amplitude weight function does not depend on any reflector property. Thus, it is possible to evaluate it for any point $(\eta, \tau)$ in the redatumed section using only information about the velocity model.

The stacking curve $\mathcal{T}_r$ is determined using two steps:

1) Given a point $(\eta, \tau)$ at the new datum, we must construct the isochron $\mathcal{Z}_{Ir}(x; \eta, \tau)$ in depth. This isochron is defined by all points $M = (x, \mathcal{Z}_{Ir}(x; \eta, \tau))$ in depth for which the sum of traveltimes along the ray segments $S_r M$ and $M G_r$, which connect the depth point $M$ to the source-receiver pair $(S_r, G_r)$, is equal to the given time $\tau$ or, mathematically,

$$T(S_r, M) + T(M, G_r) = 2T(S_r, M) = \tau \, , \tag{3}$$

where the central expression is valid for zero-offset. The traveltimes $T(S_r, M)$ and $T(G_r, M)$ depend, of course, on the available macrovelocity model.

2) In the next stage, we consider the isochron $\mathcal{Z}_{Ir}(x; \eta, \tau)$ as a reflector in an experiment with the input distribution of source-receiver pairs at the original measurement surface $z = \mathcal{Z}_l(\xi)$. The resulting

traveltime curve can be written as;

$$t = \mathcal{T}_r(\xi;\eta,\tau) = \mathcal{T}_D(\xi;x^*;z^*)\,, \tag{4}$$

where

$$\mathcal{T}_D(\xi;x^*;z^*) = T(S,M^*) + T(M^*,G) = 2T(S,M^*) \tag{5}$$

is the diffraction traveltime curve of the stationary point $M^* = (x^*, z^*)$. For each source-receiver pair at a position $\xi$, point $M^*$ represents the point on the isochron $z = \mathcal{Z}_{Ir}(x;\eta,\tau)$ where a reflection would occur that would be registered at $\xi$ with a traveltime $t$. Point $M^*$, supposed to be unique, has the coordinates $(x^*, z^* = \mathcal{Z}_{Ir}(x^*;\eta,\tau))$, where its horizontal coordinate, $x^* = x^*(\xi;\eta,\tau)$ is obtained from the stationarity condition (Fermat's principle)

$$\frac{\partial}{\partial x}\left[\mathcal{T}_D(\xi;x,z)\right]|_{x=x^*} = 0. \tag{6}$$

Pila et al. (2007b) demonstrated that the weight function $W_r(\xi;\eta,\tau)$ can be obtained from a fully analogous analysis to the one presented for migration to zero-offset (MZO) in Tygel et al. (1998). The reason is that both operations belong to the general class of configuration transforms. The arguments and mathematical derivations applied to both situations are completely analogous. The final redatuming weight function for an arbitrary medium, configuration and topography reads

$$\begin{aligned} W_r(\xi;\eta,\tau) \;=\; & \frac{v_{oS}}{v_{iS}}\sqrt{\frac{\sigma_{iS}+\sigma_{iG}}{\sigma_{oS}+\sigma_{oG}}}\,\frac{\overline{\mathcal{L}}_{iS}\overline{\mathcal{L}}_{iG}}{\overline{\mathcal{L}}_{oS}\overline{\mathcal{L}}_{oG}}\left(\frac{\cos\theta_{iS}}{\overline{\mathcal{L}}^2_{iS}}+\frac{\cos\theta_{iG}}{\overline{\mathcal{L}}^2_{iG}}\right) \\ & \frac{1}{\cos\phi}\sqrt{\frac{\cos\theta_{oR}}{v_R^3}}\,\frac{\exp\left\{i\pi[1-\mathrm{sgn}\,(K_i-Ko)]/4\right\}}{\sqrt{2|K_i-Ko|}}, \end{aligned} \tag{7}$$

where $v_{iS}$, $v_{oS}$, $v_R$ are the velocities at the sources on the input, output datums and at point $M$, respectively. Also, $\sigma_{iS}$, $\sigma_{iG}$ are the so-called optical lengths of ray segments $MS_i$ and $MG_i$, respectively, i.e., the integral of squared velocity in traveltime along the ray. Analogously, $\sigma_{oS}$, $\sigma_{oG}$, represent these factors along segments $MS_o$ and $MG_o$, respectively. These factors represent the out-of-plane geometrical-spreading factors.

The in-plane components of the geometrical spreading are given by $\overline{\mathcal{L}_{iS}}$ and $\overline{\mathcal{L}_{iG}}$, along segments $MS_i$ and $MG_i$, and $\overline{\mathcal{L}_{oS}}$ and $\overline{\mathcal{L}_{oG}}$, along segmentes $MS_o$ and $MG_o$, respectively. Moreover, symbols $\theta_{iS}$ and $\theta_{iG}$ represent the angles that the rays $M_{Si}$ and $M_{Gi}$ make with the surface normal at $S_i$ and $G_i$, respectively, and $\phi$ is the surface dip angle at $S_i$. In addition, $\theta_{oR}$ is the reflection angle at $M$ in output configuration. Finally, $K_i$ and $K_o$ are the curvatures of the input and output isochrons, respectively. For the zero-offset configuration, Pila et al. (2007b) simplified expression (7) to

$$W_r(\xi;\eta,\tau) = \frac{v_{oS}}{v_{iS}}\sqrt{2\frac{\sigma_{iS}}{\sigma_{oS}}}\,\frac{\cos\theta_s}{\cos\phi}\,\frac{1}{v_R^{3/2}\overline{\mathcal{L}}^2_{oS}}\,\frac{\exp\left\{i\pi[1-\mathrm{sgn}\,(K_i-Ko)]/4\right\}}{\sqrt{K_i-K_o}}\,, \tag{8}$$

**Homogeneous medium without topography**

For simple velocity models, the stacking curve (4) and weight function (8) can be further simplified. For example, for a homogeneous medium with a flat surface and a flat datum, i.e., $z_i(x) = 0$ and $z_r(x) = z_r$, the geometry reduces to the one depicted in Figure 1.

The stacking curve and the weight function for this case were derived by Pila et al. (2007b), resulting in

$$\mathcal{T}_r(\xi;\eta,\tau) = \frac{2}{v_o}\,(R_o+\ell) = \tau + 2\frac{\ell}{v_o} \tag{9}$$

and

$$W_r(\xi;\eta,\tau) = \sqrt{\frac{2}{v_o}}\left(\frac{R_o+\ell}{R_o}\right)\frac{z_r}{\ell^{3/2}}. \tag{10}$$

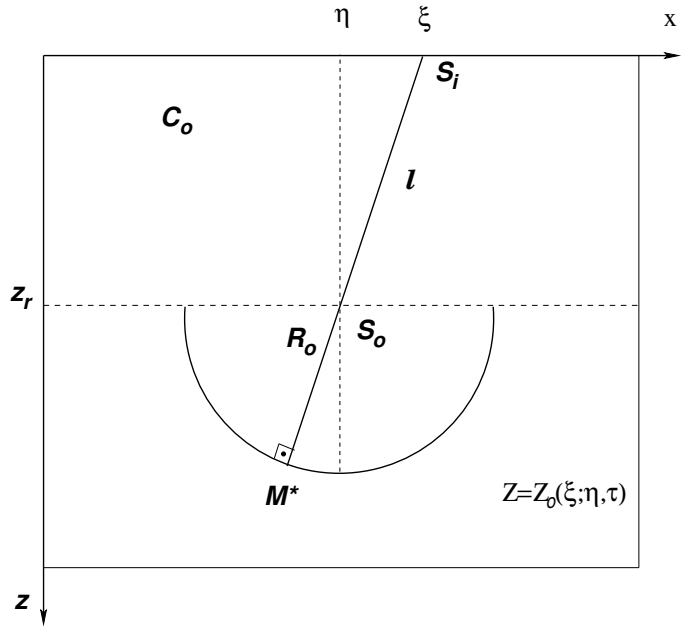


**Figure 1:** The unique reflection from an input source-receiver pair to the isochron $z = Z_o(\xi; \eta, \tau)$ crosses the center of the semicircular isochron.

### Homogeneous medium with topography

Pila et al. (2007b) have also shown how the stacking line and weight function must be modified if topography is present at the acquisition surface $z_i = z_i(\xi)$ and at the datum $z_r = z_r(\eta)$. The stacking curve (4) is still valid, with $\ell$ denoting the distance between $S_i$ and $S_o$, and in the weight function (8), the constant value $z_r$ needs to be replaced by the variable topography according to

$$z_r \rightarrow z_0 = [z_r(\eta) - z_i(\xi) - (\xi - \eta) z_i'(\xi)]\,. \tag{11}$$

No other changes are required.

## ANALYSIS OF THE VELOCITY DEPENDENCE

In this section, we study the behaviour of the redatuming operation (1) when subject to a variation of the underlying velocity model. We suppose that the operation was carried out with an erroneous velocity model $\tilde{v}$ that differs from the correct model $v$ by a certain error $\Delta v$. In the following we denote all quantities that belong to the erroneous velocity model with a tilde. For instance, the resulting wrongly redatumed data will be denoted by $\tilde{U}_r(\eta, \tau)$. To understand the error in $\tilde{U}_r(\eta, \tau)$ due to the error in the velocity field, we study the velocity derivative of the Fourier transform of equation (1),

$$U_o(\eta, \omega) = \frac{1}{\sqrt{2\pi}} \int_A d\xi W_r(\xi; \eta, \tau) e^{-i\omega \mathcal{T}_r} (i\omega)^{1/2} U_i(\xi, \omega). \tag{12}$$

We observe that in this equation, only the weight function, $W_r$, and the stacking curve, $\mathcal{T}_r$, depend on the velocity. Therefore, to understand how a velocity error $\Delta v$ affects the redatuming operation, we need to evaluate how the product $W_r e^{-i\omega \mathcal{T}_r}$ behaves under variation in $v$.

To simplify the notation, we introduce the auxiliary variable $Y$ defined as

$$Y(v) = W_r e^{-i\omega \mathcal{T}_r}. \tag{13}$$

The value $\tilde{Y}$ of this quantity for the erroneous velocity model can then be represented in a Taylor series as

$$\tilde{Y} = Y(v + \Delta v) = Y(v) + Y'(v)\Delta v + \frac{1}{2!} Y''(v)\Delta v^2 + \mathcal{O}(\Delta v^3), \tag{14}$$

where the prime denotes a derivative with respect to $v$. Substituting the first and second derivatives of $Y$ in equation (14) leads to

$$\begin{aligned} Y(v+\Delta v) &= W_r e^{-i\omega\mathcal{T}_r} - i\omega W_r e^{-i\omega\mathcal{T}_r}\frac{d\mathcal{T}_r}{dv}\Delta v + +\frac{1}{2!}(i\omega)^2 W_r e^{-i\omega\mathcal{T}_r}\left(\frac{d\mathcal{T}_r}{dv}\Delta v\right)^2 \\ &+\frac{dW_r}{dv}e^{-i\omega\mathcal{T}_r}\Delta v - i\omega\frac{dW_r}{dv}e^{-i\omega\mathcal{T}_r}\frac{d\mathcal{T}_r}{dv}\Delta v^2 \\ &+\frac{1}{2!}\left[\frac{d^2W_r}{dv^2}e^{-i\omega\mathcal{T}_r} - i\omega W_r e^{-i\omega\mathcal{T}_r}\frac{d^2\mathcal{T}_r}{dv^2}\right]\Delta v^2 + \mathcal{O}(\Delta v^3), \end{aligned} \tag{15}$$

which, upon adequate grouping of terms, yields

$$Y(v+\Delta v) \approx \left[W_r + \frac{dW_r}{dv}\Delta v\right] e^{-i\omega\mathcal{T}_r}\left[1 - i\omega\frac{d\mathcal{T}_r}{dv}\Delta v\right]. \tag{16}$$

From expression (16), we can immediately identify the resulting perturbations of the stacking line and weight function as a function of the velocity error, i.e.,

$$\Delta\tau = \frac{d\mathcal{T}_r}{dv}\Delta v \tag{17}$$

and

$$\Delta W_r = \frac{dW_r}{dv}\Delta v\,. \tag{18}$$

Interpreting the last term in equation (16) as a first-order approximation of an exponential expression, we recast that equation into the form

$$Y(v+\Delta v) \approx [W_r + \Delta dW_r]\, e^{-i\omega\mathcal{T}_r} e^{-i\omega\Delta\tau}. \tag{19}$$

Using equation (19), we can now set up the following expression for the perturbed redatumed data,

$$\tilde{U}_o(\eta,\omega) = \frac{1}{\sqrt{2\pi}}\int_A d\xi\,[W_r + \Delta dW_r]\, e^{-i\omega(\mathcal{T}_r+\Delta\tau)}(i\omega)^{1/2}U_i(\xi,\omega), \tag{20}$$

which, after an inverse Fourier transform, can be written as

$$\tilde{U}_o(\eta,\tau) = \frac{1}{\sqrt{2\pi}}\int_Y d\xi\tilde{W}_r(\xi;\eta,\tau)D^{1/2}\left[U_i(\xi,t)\right]|_{t=\tilde{\mathcal{T}}_r(\xi;\eta,\tau)}, \tag{21}$$

where

$$\tilde{W}_r(\xi;\eta,\tau) = W_r(\xi;\eta,\tau) + \Delta W_r(\xi;\eta,\tau) \tag{22}$$

and

$$\tilde{\mathcal{T}}_r(\xi;\eta,\tau) = \mathcal{T}_r(\xi;\eta,\tau) + \Delta\tau = \mathcal{T}_r(\xi;\eta,\tau-\Delta\tau) \tag{23}$$

describe the perturbed weight function and stacking line with a velocity error $\Delta v$. The second equality in equation (23) means that a redatuming with an erroneous velocity $\tilde{v}$ will position the event at the same position as if redatumed with the true velocity $v$ at a different output time $\tau-\Delta\tau$, with $\Delta\tau$ given in equation (17). Since the stationary value of integral (21) is the one that determines the output $\tilde{U}_o$, this shifted event will have its amplitude perturbed by $\Delta W$ as given by equation (18). In other words, if an estimate of the velocity error $\Delta v$ is available, it is possible to correct the redatumed data directly. The correction term for the phase is directly given by equation (17). The correction term for the amplitude combines equation (18) with additional corrections for the different traveltime Hessians and the dislocation of the stationary point.

**Quantitative analysis**

For the special cases discussed earlier, we can perform a more quantitative analysis of the perturbations. We start with the weight function (10), which can be rewritten as

$$W_r(\xi;\eta,\tau) = \sqrt{\frac{2}{v}}\left(\frac{v\tau+2\ell}{v\tau}\right)\frac{z_0}{\ell^{3/2}}, \tag{24}$$

where we have used that $R_0 = \frac{v\tau}{2}$, with $\tau$ being the fixed output time. Thus, we find

$$\begin{aligned}\frac{d}{dv}\left(W_r(\xi;\eta,\tau)\right) &= \frac{d}{dv}\left(\sqrt{\frac{2}{v}}\left(1+\frac{2\ell}{v\tau}\right)\frac{z_0}{\ell^{3/2}}\right)\\ &= -\frac{1}{2}v^{-3/2}\sqrt{2}\left(1+\frac{2\ell}{v\tau}\right)\frac{z_0}{\ell^{3/2}} - \sqrt{\frac{2}{v}}\frac{2\ell}{v^2\tau}\frac{z_0}{\ell^{3/2}},\end{aligned} \tag{25}$$

which yields

$$\Delta W_r(\xi;\eta,\tau) = -\frac{\Delta v}{2v}W_r - \sqrt{\frac{2}{v}}\left(\frac{\ell}{R_0}\right)\frac{z_0}{\ell^{3/2}}\frac{\Delta v}{v}. \tag{26}$$

This equation shows that we must expect an amplitude reduction if the redatuming is carried out with a too high velocity ($\Delta v > 0$) and vice versa. If $\ell \ll R_0$, i.e., the datum is close to the acquisition surface, the second term in equation (26) can be neglected. Then, the relative amplitude error can be estimated from

$$\frac{\Delta W_r(\xi;\eta,\tau)}{W_r} \approx -\frac{1}{2}\frac{\Delta v}{v}, \tag{27}$$

i.e., the amount of the relative amplitude error is about half the amount of the relative velocity error. On the other hand, if $\ell \gg R_0$, i.e., if the datum is close to the reflector, then $R_0 + \ell \approx \ell$ in equation (24). In that case, the relative amplitude error is approximately given by

$$\frac{\Delta W_r(\xi;\eta,\tau)}{W_r} \approx -\frac{3}{2}\frac{\Delta v}{v}, \tag{28}$$

i.e., the amount of the relative amplitude error is about one-and-a-half times the amount of the relative velocity error. Finally, if $\ell \approx R_0$, i.e., the datum is about half way down to the reflector, the relative amplitude error can be approximated by

$$\frac{\Delta W_r(\xi;\eta,\tau)}{W_r} \approx -\frac{\Delta v}{v}, \tag{29}$$

i.e., the relative amplitude error is of about the same size as the relative velocity error.

The inclusion of topography, which requires the modification of the weight function as indicated in equation (11), does not alter the analysis above.

To estimate the phase error, we start from equation (9). Taking its $v$ derivative yieds

$$\frac{d}{dv}\left(\mathcal{T}_r\right) = \frac{d}{dv}\left(\tau + \frac{2\ell}{v}\right) = \frac{-2\ell}{v^2}. \tag{30}$$

Thus, the phase error is given by

$$\Delta\mathcal{T}_r = \frac{-2\ell}{v^2}\Delta v. \tag{31}$$

We observe that the phase shift for a positive velocity error is negative. In other words, the redatumed event will appear later in the redatumed section than with the correct velocity. In the case of $\ell \gg R_0$, equation (31) can be approximated as

$$\frac{\Delta\mathcal{T}_r}{\mathcal{T}_r} \approx -\frac{\Delta v}{v}, \tag{32}$$

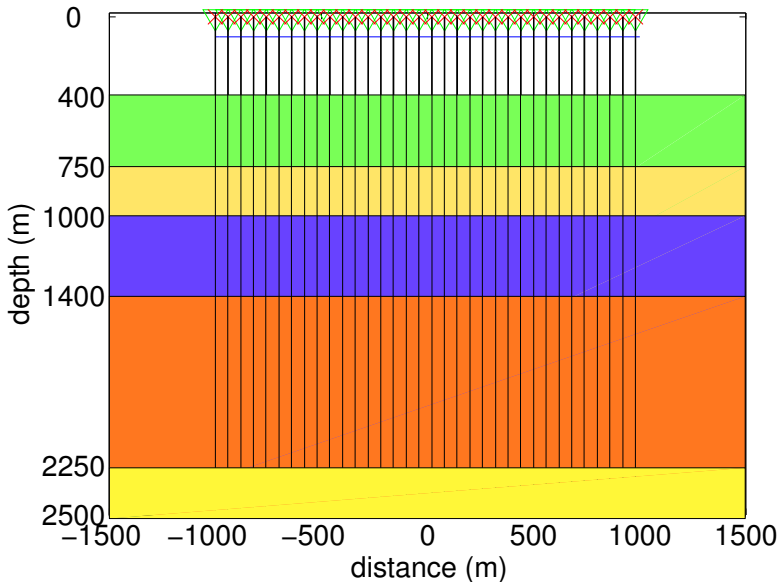


**Figure 2:** Model for the first numerical experiment: A zero- offset experiment was simulated at z = 0 above set of plain reflectors. Also shown is the datum level (blue line) at $z = 100$ m.

i.e., the size of the relative phase error corresponds to that of the relative velocity error. For $\ell \approx R_0$, we find

$$\frac{\Delta \mathcal{T}_r}{\mathcal{T}_r} \approx -\frac{1}{2}\frac{\Delta v}{v}, \tag{33}$$

i.e., the relative phase error amounts to half the relative velocity error. Finally, for $\ell \ll R_0$, we observe from equation (9) that $\mathcal{T}_r \ll 2\ell/v$, which implies that

$$\left|\frac{\Delta \mathcal{T}_r}{\mathcal{T}_r}\right| \ll \left|\frac{\Delta v}{v}\right|. \tag{34}$$

From this analysis, we conclude that the relative phase error should be very small for a datum close to the acquisition surface and should never exceed the size of the relative velocity error.

## NUMERICAL EXPERIMENTS

### Inhomogeneous models

The validity of the theory was confirmed by Pila et al. (2007b) by numerical tests using homogeneous models. In this work, we investigate the velocity dependence of the redatuming operation by applying it to slightly more complicated models.

**First model** In the first synthetic experiment, we apply constant-velocity redatuming to a horizontally layered model with five horizontal layers with acoustic wave velocitys of 1500 m/s, 1800 m/s, 2500 m/s, 3300 m/s, and 4000 m/s. Figure I shows the geometry of the reflectors together with the ray family of the zero-offset configuration. The source-receiver pairs are positioned at $z = 0$ m at every 20 m between $\xi = -1000$ m and $\xi = 1000$ m. Also show in Figure I is the new datum level at $z = 100$ m (blue line). We generated the synthetic data using Kirchhoff modelling in the RMS velocity model (see Figure I). These data have then been used as input for redatuming operation (1), with stacking line (9) and weight function (10) using the correct RMS velocity model. The output configuration also consists of source-receiver pairs at every 20 m between $\eta = -1000$ m and $\eta = 1000$ m. The resulting redatumed data are depicted in Figure 4. For comparison, Figure 5 shows the ideal result of this redatuming operation, i.e., the section obtained by direct Kirchhoff modelling at the datum level. Comparing Figures 4 and 5, we recognize that the kinematic transformation was very good. The structure of the redatumed reflection data looks identical

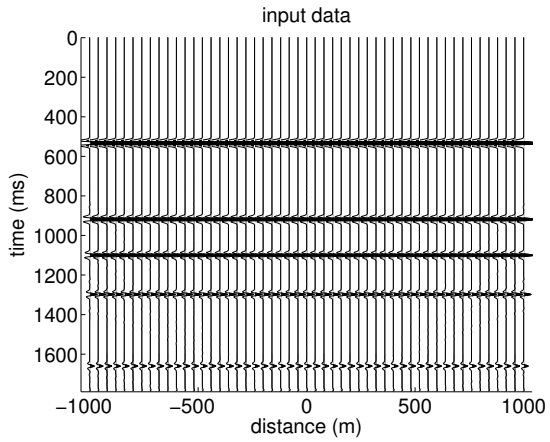


**Figure 3:** Modeled seismic zero-offset section as input to redatuming.

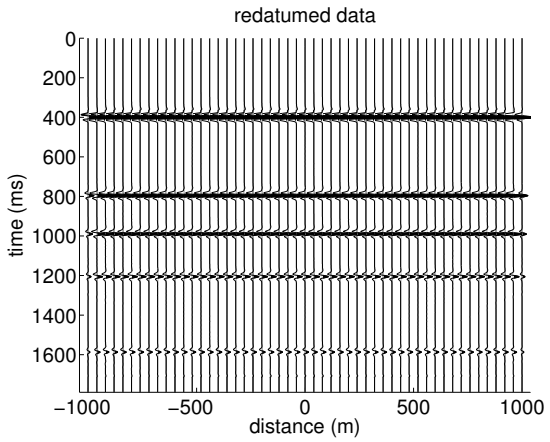


**Figure 4:** Section resulting from redatuming operation (1) to $z = 100$ m.

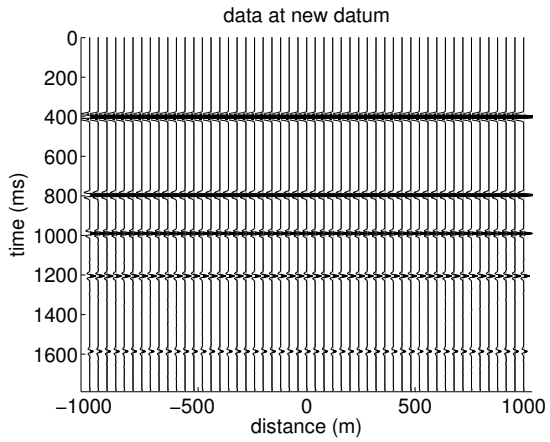


**Figure 5:** Section resulting from Kirchhoff modelling at $z = 100$ m. Note that the redatumed section in Figure 4 looks almost identical to this reference section.

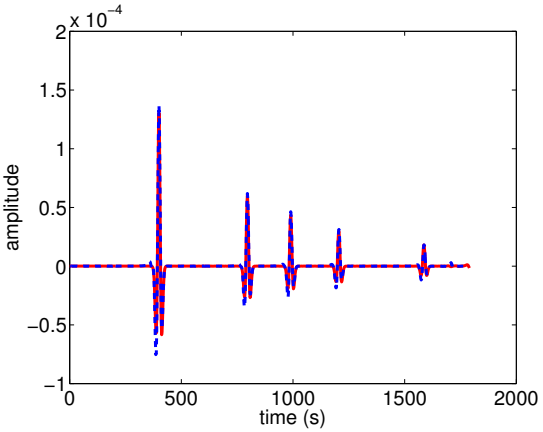


**Figure 6:** Comparison of the central traces of Figures 4 and 5. Notice the good coincidence between the redatumed (dashed line) and modelled (continuous line) traces.

to the one of the modelled data. Also, the amplitudes of the five events are correctly recovered. Some operator noise is visible after the events. For a more detailed appreciation of the quality of the redatumed data, Figure 6 shows a comparison of the central traces of Figures 4 and 5. We see that the five events are well recovered.

**Second model** In the second synthetic test, the acquisition surface and datum have different sinusoidal topographies (see Figure 7). The model consists of two homogeneous and isotropic flat layers with acoustic wave velocitys of 1500 m/s and 1800 m/s. Figure 7 shows the geometry of the reflector together with the ray family of the zero-offset configuration. The source-receiver pairs are positioned at every 20 m between $\xi = -1000$ m and $\xi = 1000$ m. Also show in Figure 7 is the new datum surface at $z = z_r(\eta)$ (blue line).

The synthetic Kirchhoff data for the model in Figure 7 are depicted in Figure 8. They have then been used as an input for single-stack redatuming according to operation (1). The output configuration also consists of source-receiver pairs at every 20 m between $\eta = -1000$ m and $\eta = 1000$ m. The data resulting from redatuming are depicted in Figure 9. For comparison, Figure 10 shows the ideal result of this redatuming operation. The section in Figure 10 was obtained by direct Kirchhoff modelling at the datum level. Comparing Figures 9 and 10, we recognize that the kinematic transformation was very good. The structure of the redatumed reflection data looks identical to the one of the modelled data. Some operator noise is visible after the event. For a more quantitative comparison, Figure 11 compares the central traces of the modelled and redatumed sections in Figures 8 and 9. We notice the almost perfect coincidence

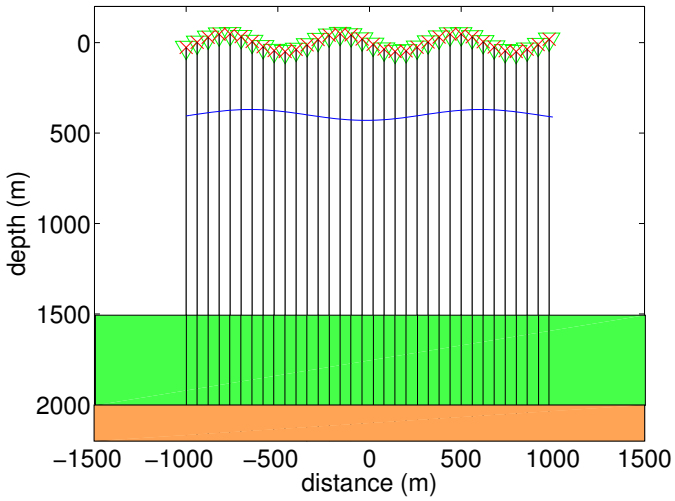


**Figure 7:** Model for the second numerical experiment: A zero-offset experiment was simulated at $z_i =$ [illegible]

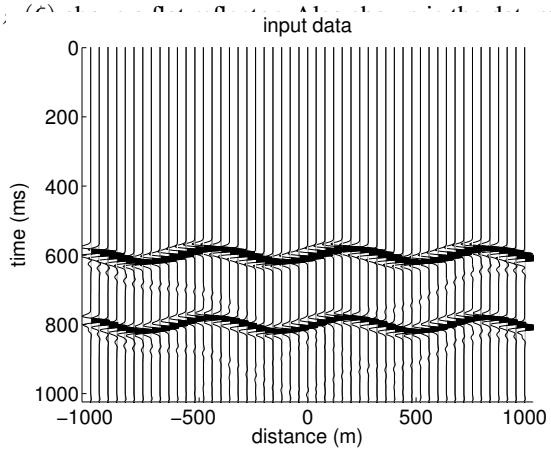


**Figure 8:** Modeled seismic zero-offset section.

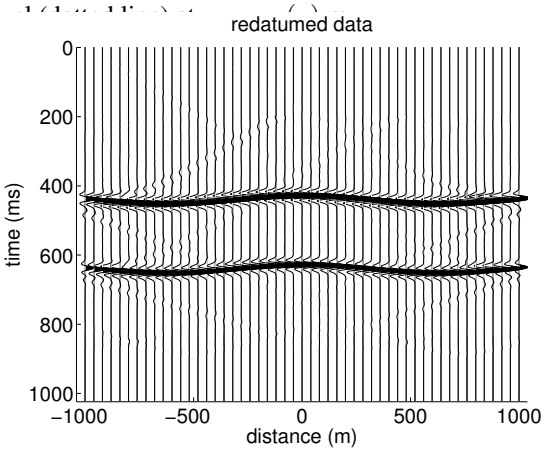


**Figure 9:** Section resulting from redatuming to $z_r$.

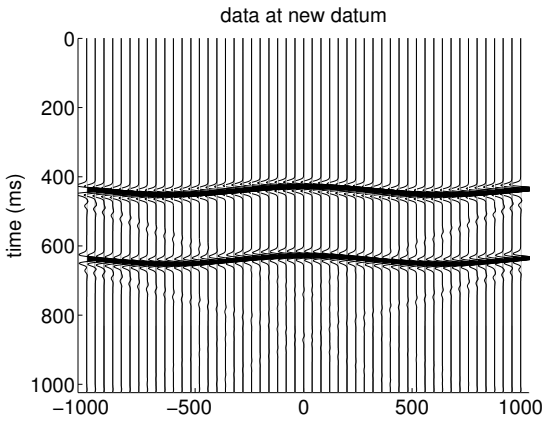


**Figure 10:** Section resulting from Kirchhoff modelling at $z_r(\eta)$. Note that the redatumed section in Figure 9 looks almost identical to this reference section.

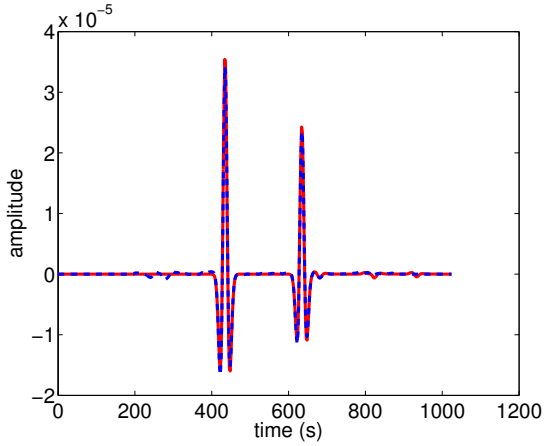


**Figure 11:** Comparison of the central traces of Figures 9 and 10. Notice the good coincidence between the redatumed (dashed line) and modelled (continuous line) traces.

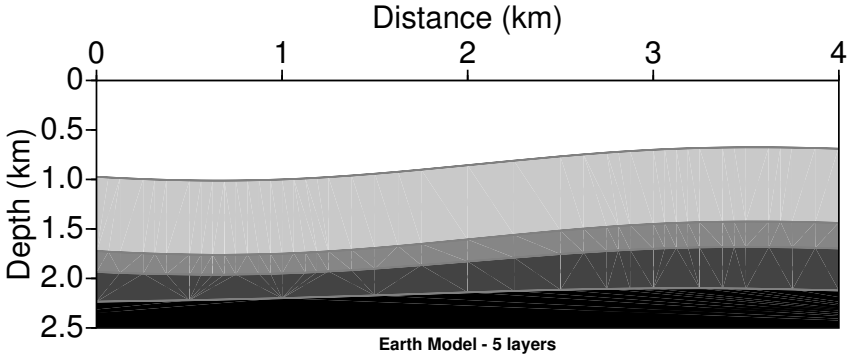


**Figure 12:** Laterally inhomogeneous model for the third synthetic experiment.

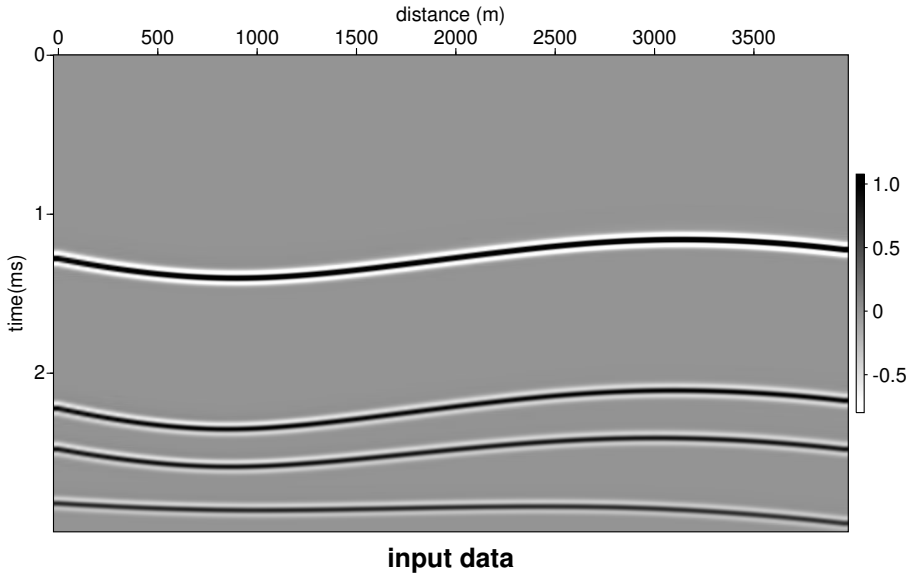


**Figure 13:** Modeled seismic zero-offset section.

between the redatumed (dashed line) and modelled (continuous line) traces.

**Model with lateral velocity variations** The third model consists of four smoothly curved interfaces separating homogeneous layers with velocities 1508 m/s, 1581 m/s, 1690 m/s, 1826 m/s, and 2000 m/s (Figure 12). We modelled synthetic zero-offset data by Gaussian beams at the planar surface with source-receiver pairs at every 50 m between $\xi = 0$ m and $\xi = 4000$ m (Figure 13). Then, we redatumed these data to a depth of $z_r = 100$ m (Figure 14) using the velocity of the topmost layer and compared them to data modelled at the datum level (Figure 15). The two sections look almost identical. While the first three events are virtually undistinguishable in the modelled and redatumed sections, some amplitude loss can be observed at the deepest event.

### Velocity error

To test the prediction of the theoretical analysis of the velocity dependence, we generated synthetic data in the model depicted in Figure 16. It consists of a planar reflector below a homogeneous overburden with velocity 5000 m/s. The source-receiver pairs cover a sinusoidal acquisition surface with $z_i = 50\sin(\xi/150)$ m at every 10 m. The datum is another sinusoidal surface at about 400 m depth with $z_r = 30\sin(\xi/200 - 80) + 400$ m. Figures 17, 18, and 19 show the input data, the redatumed data and synthetic reference data modelled at the datum level.

The phase and amplitude error of the redatumed event are shown in Figures 20 and 21. Our next step was to perturb the velocity used for the redatuming with a 15% error. After this perturbation, the phase and

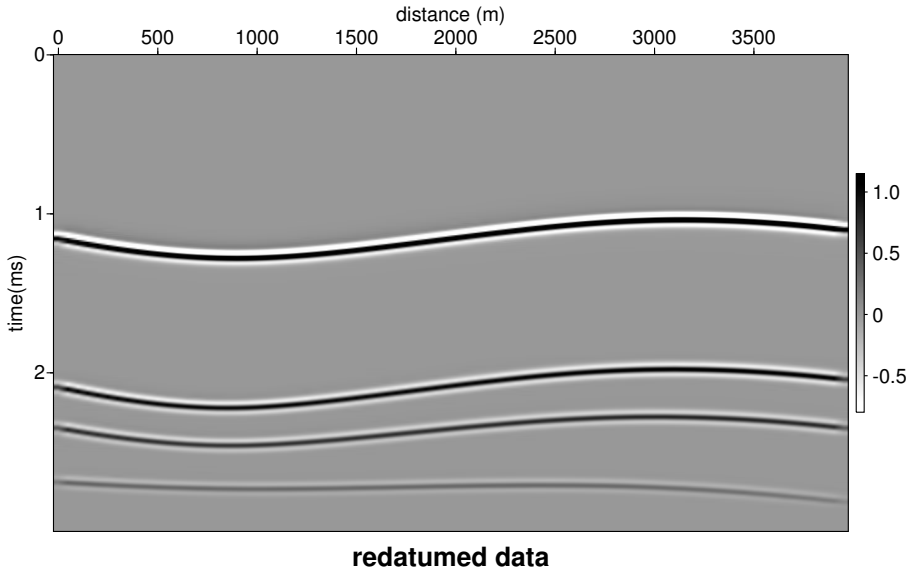


**Figure 14:** Section resulting from redatuming to $z = 100\ m$

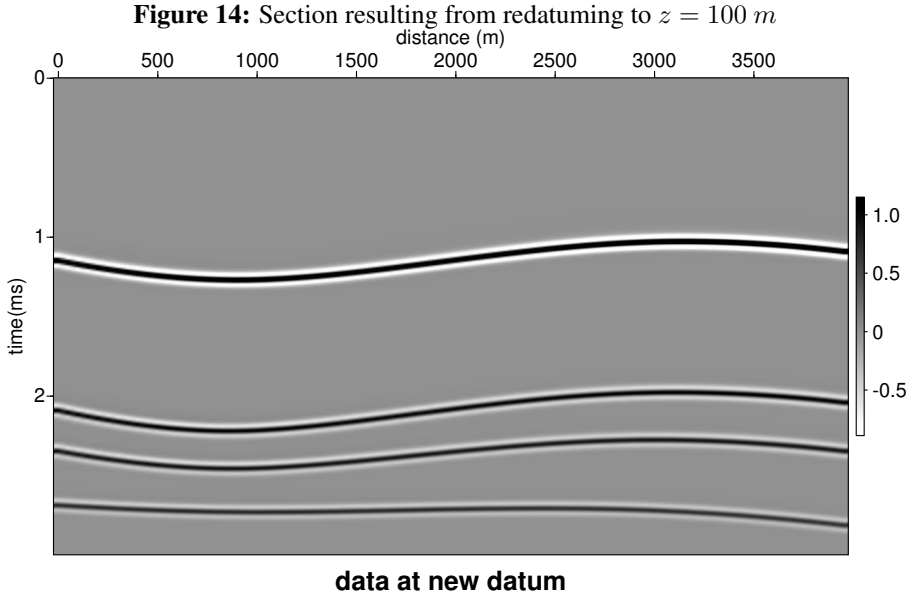


**Figure 15:** Section resulting from modelling at $z = 100\ m$

amplitude errors increase, as shown in Figures 22 and 23. However, a correction using formulas (17) and (18) reduces these errors (Figures 24 and 25) to the same order as the ones obtained with the true model velocity (Figures 20 and 21).

## CONCLUSIONS

The redatuming operation can be thought of as being composed of a true-amplitude diffraction-stack migration and true-amplitude isochron-stack demigration, as described in the unified approach to seismic reflection imaging (Hubral et al., 1996; Tygel et al., 1996). Based on this observation, Pila et al. (2007b) derived analytic expressions for the stacking line and weight function of single-stack redatuming.

This particular way of deriving the single-stack redatuming operator points towards its potential dependence on the velocity model. In this work, we have studied this velocity dependence. We have seen that a velocity error causes amplitude and phase errors that are expected to be of approximately the same size as the velocity errors. The phase of redatumed data turned out to be more robust than their amplitude. Our

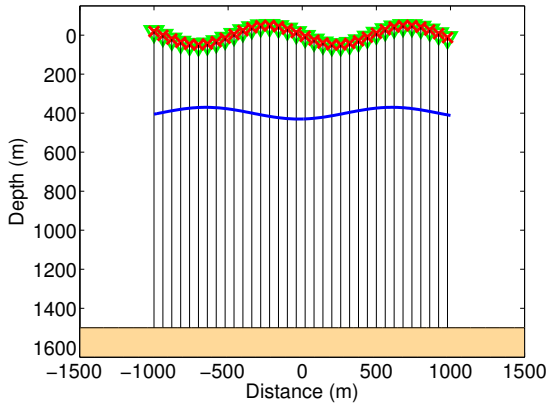


**Figure 16:** Model for the velocity error test. The original acquisition surface and the datum (blue line) are sinusoidal surfaces.

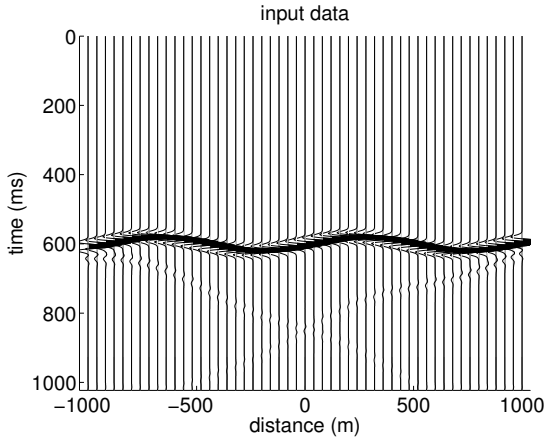


**Figure 17:** Synthetic zero-offset section obtained from Kirchhoff modelling at the original sinusoidal acquisition surface of Figure 16.

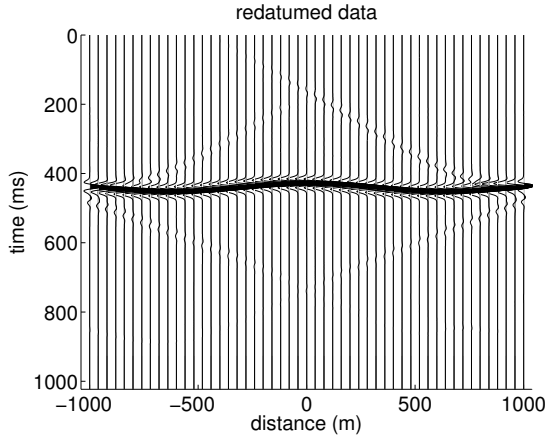


**Figure 18:** Redatumed section at the sinusoidal datum of Figure 16.

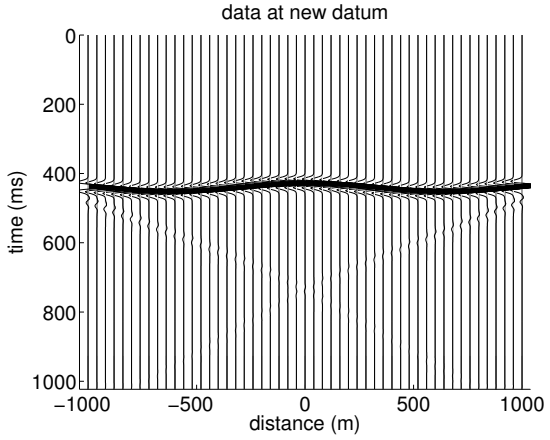


**Figure 19:** Modelled section at the sinusoidal datum of Figure 16.

theoretical analysis led to amplitude and phase factors that allow for a direct correction of the redatumed data, if an estimate of the velocity error is available.

Moreover, we have applied the redatuming operator of Pila et al. (2007b) to different synthetic data for models with two or more layers and in models with lateral velocity variations. In these experiments, we have seen that seismic data acquired at the measurement surface were repositioned correctly to a new level, preserving attributes as amplitude and phase. The topography did not present a restriction to the application of the method. Application with slightly wrong velocity models did not cause a significant error in the redatumed data.

Further investigations are being carried to test the potential of the redatuming operator for applications in models with stronger lateral velocity variations.

## ACKNOWLEDGMENTS

This work has been partially supported by the National Council of Scientific and Technological Development (CNPq), Brazil, as well as Petrobras and the sponsors of the Wave Inversion Technology (WIT) Consortium, Germany.

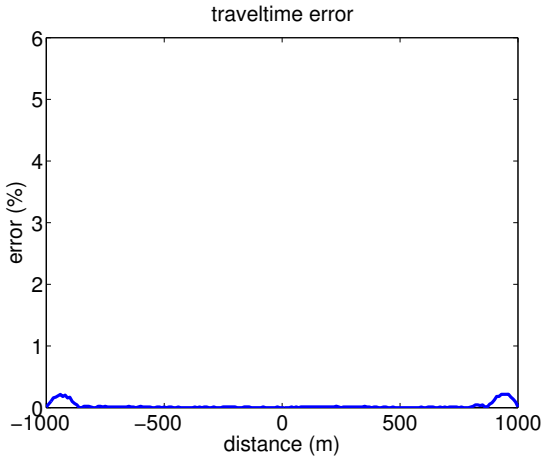


**Figure 20:** Traveltime error of redatuming using the correct velocity.

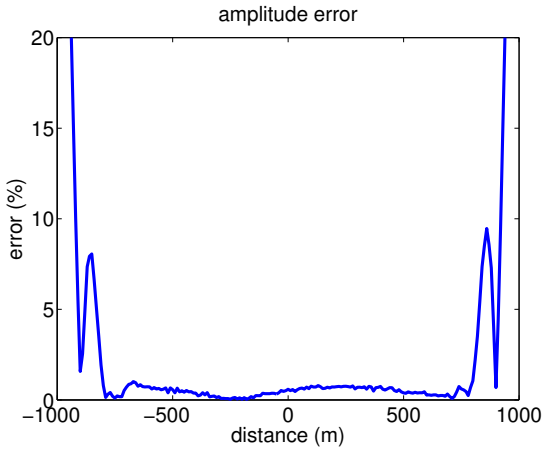


**Figure 21:** Amplitude error of redatuming using the correct velocity.

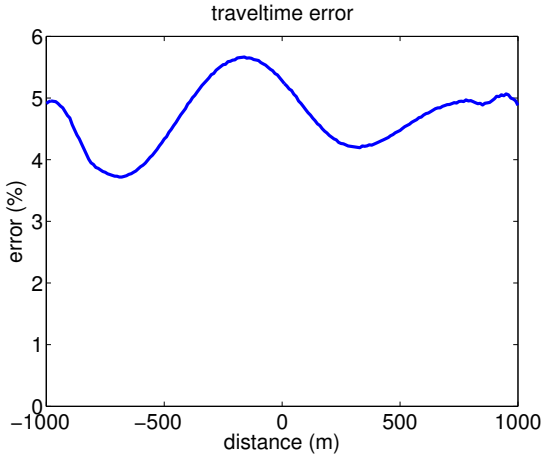


**Figure 22:** Traveltime error of redatuming using a 15% too high velocity.

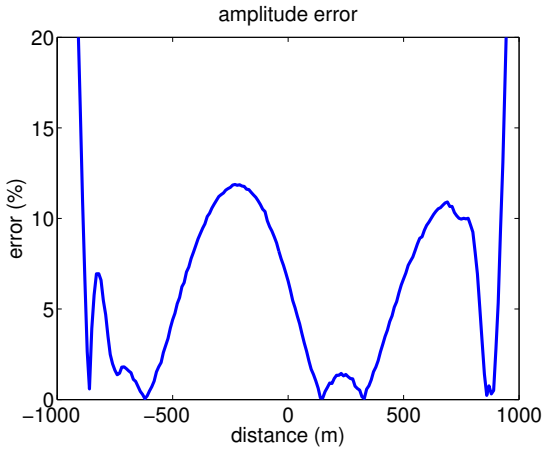


**Figure 23:** Amplitude error of redatuming using a 15% too high velocity.

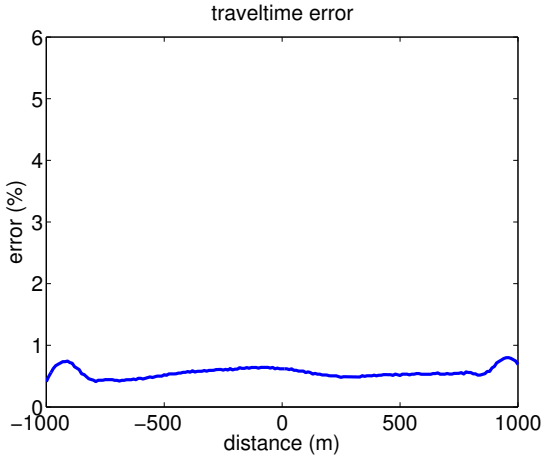


**Figure 24:** Traveltime error after phase correction.

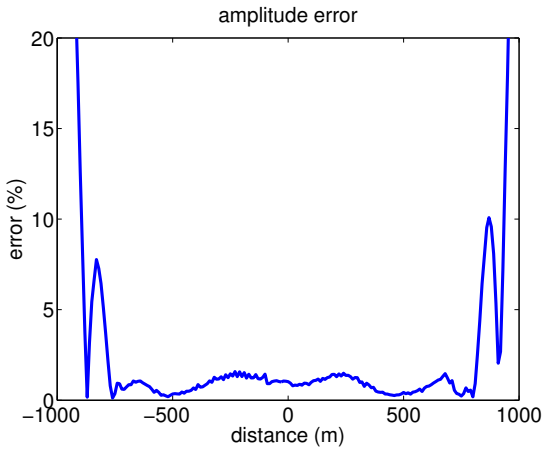


**Figure 25:** Amplitude error after correction.

## REFERENCES

Berryhill, J. R. (1979). Wave-equation datuming. *Geophysics*, 44(8):1329–1344.

Berryhill, J. R. (1984). Wave-equation datuming before stack. *Geophysics*, 49(11):2064–2066.

Berryhill, J. R. (1986). Submarine canyons: Velocity replacement by wave-equation datuming before stack. *Geophysics*, 51(8):1572–1579.

Bevc, D. (1997). Flooding the topography: Wave-equation datuming of land data with rugged acquisition topography. *Geophysics*, 62(05):1558–1569.

Bleistein, N. (1986). Two-and-one-half dimensional in-plane wave propagation. *Geophysical Prospecting*, 34(5):686–703.

Hanitzsch, C., Schleicher, J., and Hubral, P. (1994). True-amplitude migration of 2D synthetic data. *Geophys. Prosp.*, 42(5):445–462.

Hubral, P., Schleicher, J., and Tygel, M. (1996). A unified approach to 3-D seismic reflection imaging – Part I: Basic concepts. *Geophysics*, 61(3):742–758.

Pila, M., Schleicher, J., and Novais, A. (2007a). True amplitude diffraction-stack redatuming. In *Expanded Abstracts, 10th Internat. Congress*, pages 1–4, Rio de Janeiro, Brazil. SBGf.

Pila, M. F., Schleicher, J., and Novais, A. (2007b). 2.5D true-amplitude diffraction-stack redatuming. *WIT consortium, Annual Report*, 11:149–162.

Schleicher, J., Tygel, M., and Hubral, P. (1993). 3-D true-amplitude finite-offset migration. *Geophysics*, 58(8):1112–1126.

Schleicher, J., Tygel, M., and Hubral, P., editors (2007). *Seismic True-Amplitude Imaging*. Number 12 in Geophysical Developments. SEG.

Schneider, W. A., Phillip, L. D., and Paal, E. F. (1995). Wave-equation velocity replacement of the low-velocity layer for overthrust-belt data. *Geophysics*, 60(2):573–579.

Schuster, G. T. and Zhou, M. (2006). A theoretical overview of model-based and correlation-based redatuming methods. *Geophysics*, 71(4):SI103–SI110.

Tygel, M., Schleicher, J., and Hubral, P. (1996). A unified approach to 3-D seismic reflection imaging – Part II: Theory. *Geophysics*, 61(3):759–775.

Tygel, M., Schleicher, J., Hubral, P., and Santos, L. T. (1998). 2.5-D true-amplitude Kirchhoff migration to zero offset in laterally inhomogeneous media. *Geophysics*, 63(2):557–573.

Wapenaar, C. P. A., Cox, H. L. H., and Berkhout, A. J. (1992). Elastic redatuming of multicomponent seismic data. *Geophysical Prospecting*, 40(4):465–482.

Yilmaz, O. and Lucas, D. (1986). Prestack layer replacement. *Geophysics*, 51(7):1355–1369.